Table S1. Characteristics of healthy patients and patients with non-alcoholic fatty liver disease related to Figures 1 and 2

Variable	Healthy (N=9)	NAFLD (N=11)	*P*-value
Age (Years)			
Mean (± SD)	34.56 (± 6.41)	48.18 (± 12.26)	**0.008**
Gender			
Male	6 (66.67)	4 (36.36)	0.370
Female	3 (33.33)	7 (63.64)	
Race/Ethnicity			
Caucasian	2 (22.22)	6 (54.55)	**0.008**
African American	0 (0)	1 (9.09)	
Asian	7 (77.78)	1 (9.09)	
Other	0 (0)	3 (27.27)	
ALT (U/L)			
Median (± SD)	30.22 (± 9.58)	29.91 (± 18.05)	0.963
AST (U/L)			
Mean (± SD)	27 (± 6.65)	23.27 (± 7.95)	0.277
BMI (kg/m^2)			
Mean (± SD)	21.56 (± 1.75)	36.94 (± 7.12)	**< 0.001**
Fatty liver			
0	9 (100)	0 (0)	NA
< 33%	0 (0)	7 (63.64)	
33–66%	0 (0)	3 (27.27)	
> 66%	0 (0)	1 (9.09)	

Data are presented as number of patients (%), mean (± SD), or median (IQR).
p-values were calculated by two-sample t-test or Mann-Whitney test for continuous variables and by chi-squared test or Fisher's exact test for categorical variables, as appropriate.
[a]ALT, alanine aminotransferase; AST, aspartate aminotransferase; BMI, body mass index; IQR, interquartile range; NA, not applicable; NAFLD, non-alcoholic fatty liver disease; SD, standard deviation.

Table S2. Characteristics of patients with and without non-alcoholic fatty liver disease related to Figure 7A and 7B.

Variable	Normal (N=18)	NAFLD (N=16)	*P*-value
Age at Biopsy (Years)			
Mean (± SD)	54.22 (± 15)	61.56 (± 12.15)	0.130
Gender			
Male	11 (61.11)	9 (56.25)	0.774
Female	7 (38.89)	7 (43.75)	
Race/Ethnicity			
Caucasian	10 (55.56)	9 (56.25)	0.361
African American	0 (0)	2 (12.5)	
Asian	4 (22.22)	1 (6.25)	
Other	4 (22.22)	4 (25)	
Chemotherapy			
Yes	14 (77.78)	14 (87.5)	0.660
No	4 (22.22)	2 (12.5)	
BMI (kg/m^2)			
Median (IQR)	23.43 (21.46–26.22)	28.19 (25.3–34.55)	**0.003**
Fatty liver			
0	18 (100)	0 (0)	NA
< 33%	0 (0)	10 (62.5)	
33–66%	0 (0)	1 (6.25)	
> 66%	0 (0)	5 (31.25)	

Data are presented as number of patients (%), mean (± SD), or median (IQR).
p-values were calculated by two-sample t-test or Mann-Whitney for continuous variables and by chi-squared test or Fisher's exact test for categorical variables, as appropriate.
[a]BMI, body mass index; IQR, interquartile range; NA, not applicable; SD, standard deviation.

Table S3. Characteristics of patients with and without non-alcoholic fatty liver disease related to Figure 7C–G.

Variable	Normal (N=17)	NAFLD (N=13)	*P*-value
Age at Biopsy (Years)			
Mean (± SD)	55.18 (± 15.48)	59.23 (± 11.5)	0.436
Gender			
Male	11 (64.71)	6 (46.15)	0.310
Female	6 (35.29)	7 (53.85)	
Race/Ethnicity			
Caucasian	8 (47.06)	6 (46.15)	0.526
African American	0 (0)	2 (15.38)	
Asian	3 (17.65)	1 (7.69)	
Other	6 (35.29)	4 (30.77)	
Chemotherapy			
Yes	13 (76.47)	11 (84.62)	0.672
No	4 (23.53)	2 (15.38)	
BMI (kg/m^2)			
Median (IQR)	22.91 (21.46–25.92)	29.29 (25.27–34.77)	**0.003**
Fatty liver			
0	17 (100)	0 (0)	NA
< 33%	0 (0)	8 (61.54)	
33–66%	0 (0)	1 (7.69)	
> 66%	0 (0)	4 (30.77)	

Data are presented as number of patients (%), mean (± SD), or median (IQR).
p-values were calculated by two-sample t-test or Mann-Whitney test for continuous variables and by chi-squared test or Fisher's exact test for categorical variables, as appropriate.
[a]BMI, body mass index; IQR, interquartile range; NA, not applicable; SD, standard deviation.

Table S4. Antibody list for Imaging Mass Cytometry analysis of Human Colorectal Cancer and Liver Metastasis related to Figure 7

	Metal	Antibody	Clone	Cell subsets	Vendor	Cat #
1	113In	aSMA	1A4/ASM-1	myofibroblast	Novus Biologicals	NBP2-34522
2	115In	CD31	C31.3	endothelium, vessels	Abcam	ab212709
3	142Nd	Galectin-9	1G3	TIM3 ligand	EMD Millipore	MABT833
4	143Nd	YAP1	EP1674Y	tumor marker	Abcam	ab172373
5	144Nd	CD14	EPR3653	monocyte, macrophage	Fluidigm	3144025D
6	145Nd	Cytokeratin 19	RCK108	cytokeratin, bile ducts	Novus Biologicals	NBP1-97712
7	147Sm	CD163	EDHu-1	M2 macrophage	Fluidigm	3147021D
8	148Nd	NKG2D	pAb	NK cells	Novus Biologicals	NBP2-43645
9	150Nd	PDL1	28-8	immunoregulatory	Abcam	ab228413
10	151Eu	FAP	pAb	CaF	R&D Systems	AF3715
11	152Sm	CD11c	ITGAX/1242	DC	Abcam	ab212508
12	153Eu	LAG-3	D2G40	immunoregulatory	Fluidigm	3153028D
13	154Sm	HepPar1	HepPar1/V3109	hepatocyte	NSJ Bioreag	V3109SAF
14	155Gd	FOXP3	236A/E7	Treg	Fluidigm	3155016D
15	156Gd	CD4	EPR6855	T helper	Fluidigm	3156033D
16	159TB	CD68	KP1	macrophages	Fluidigm	3159035D
17	160Gd	VISTA	D1L2G	myeloid checkpoint	Fluidigm	3160025D
18	161Dy	CD20	H1	B cells	Fluidigm	3161029D
19	162Dy	CD8a	C8/144B	cytotoxic T cells	Fluidigm	3162034D
20	163Dy	TIM3	D5D5R	immunoregulatory	Cell Signaling Tech	81229SF
21	165Ho	PD1	NAT105	immunoregulatory	Abcam	ab201811
22	166Er	iNOS	SP126	M1 macrophage/hepatocyte	Abcam	ab239990
23	168Er	CDX-2	2951R	tumor marker	Novus Biologicals	NBP3-08738
24	170Er	CD3	pAb	pan T-cell	Fluidigm	3170019D
25	172Yb	CD15	HI98	myeloid, granulocytes	Biolegend	301902
26	173Yb	CD11b	EPR1344	macrophages	Abcam	ab209970
27	196Pt	Ki-67	B56	proliferation	BD Biosciences	556003
28	209Bi	Histone H3	EPR16987	nuclear	Abcam	ab238971
29	89Y	CD45	D9M8I	pan leukocytes	Cell Signaling Tech	47937
30	139La	HLA-ABC	EMR8-5	MHC class I	Abcam	Ab70328
31	174Yb	HLA-DR	L243	MHC class II, MDSC, APC	Fluidigm	3174023D

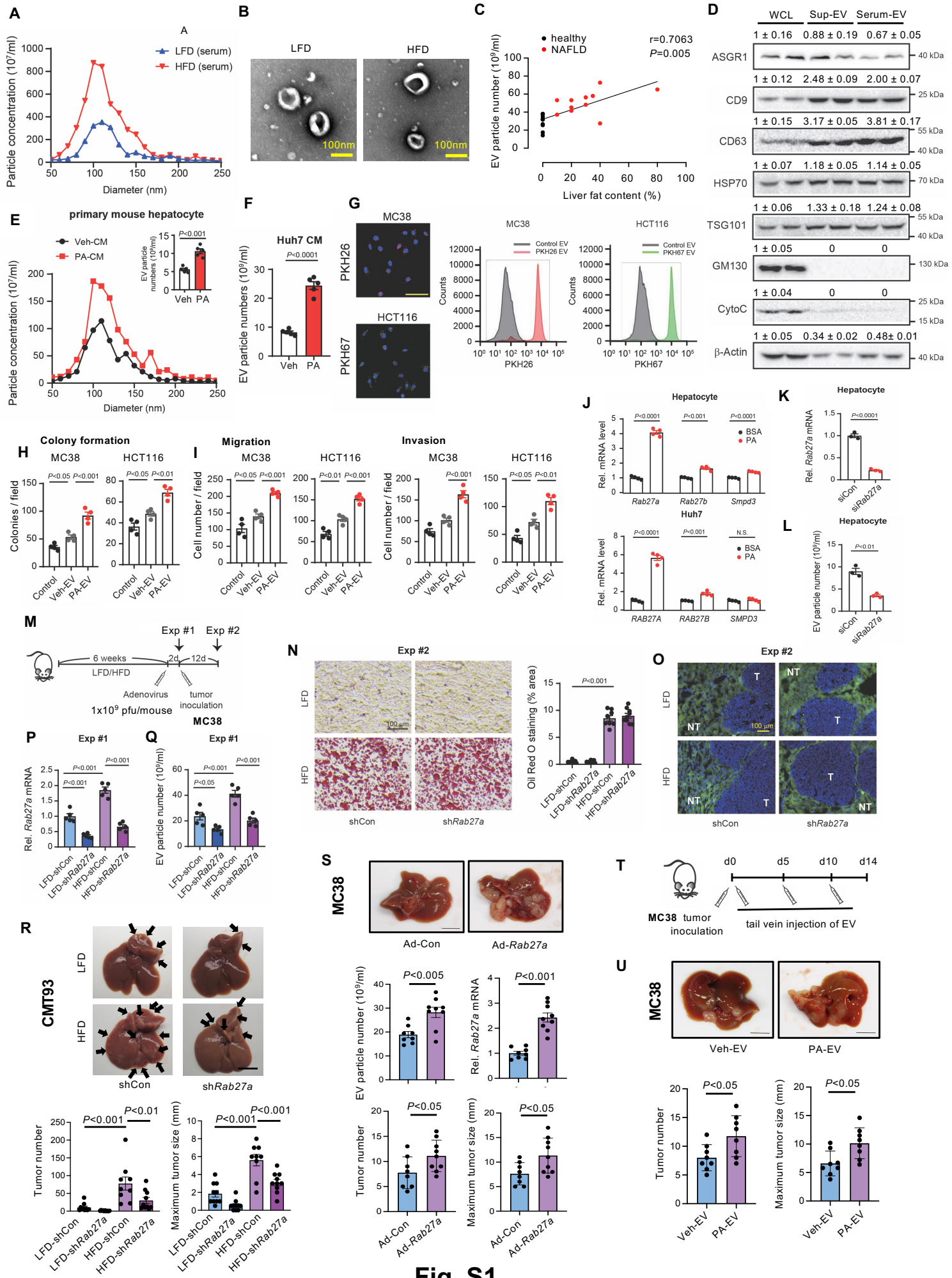
A
B
C
D
E
F
G
H
I
J
K
L
M
N
O
P
Q
R
S
T
U
LFD (serum)
HFD (serum)
Particle concentration (10^7/ml)
Diameter (nm)
LFD
HFD
100nm
healthy
NAFLD
r=0.7063
P=0.005
EV particle number (10^9/ml)
Liver fat content (%)
WCL
Sup-EV
Serum-EV
ASGR1
CD9
CD63
HSP70
TSG101
GM130
CytoC
β-Actin
40 kDa
25 kDa
55 kDa
70 kDa
130 kDa
15 kDa
primary mouse hepatocyte
Veh-CM
PA-CM
Huh7 CM
MC38
HCT116
PKH26
PKH67
Control EV
PKH26 EV
PKH67 EV
Counts
Hepatocyte
Huh7
BSA
PA
Rel. mRNA level
Rab27a
Rab27b
Smpd3
RAB27A
RAB27B
SMPD3
siCon
siRab27a
Colony formation
Migration
Invasion
Colonies / field
Cell number / field
Control
Veh-EV
PA-EV
6 weeks
LFD/HFD
Exp #1
Exp #2
2d
12d
Adenovirus
1x10^9 pfu/mouse
tumor inoculation
Oil Red O staining (% area)
shCon
shRab27a
LFD-shCon
LFD-shRab27a
HFD-shCon
HFD-shRab27a
CMT93
Tumor number
Maximum tumor size (mm)
Ad-Con
Ad-Rab27a
d0
d5
d10
d14
MC38 tumor inoculation
tail vein injection of EV
Veh-EV
PA-EV

Fig. S1

Figure S1. Increased Extracellular Vesicle Release by Fatty Liver Enhances Metastatic Tumor Growth in the Liver, Related to Figure 1

(A) Particle size distribution of EVs assessed using a qNANO instrument. Mouse sera were obtained by the procedure outlined in Figure 1A.

(**B**) Transmission electron microscopy images of EVs from PHCs of LFD and HFD-fed mice.

(**C**) The correlation between serum EV particle number and liver fat content in healthy and NAFLD patients.

(**D**) Immunoblots and quantifications of lysates of mouse PHCs (WCL), EVs from supernatants of mouse PHCs (Sup-EV), and EVs from mouse serum (Serum-EV).

(**E**) Numbers of EV particles obtained from supernatants of Huh7 cells treated with Veh or 400 μM PA for 24 hours (n=5/group) were assessed using a qNANO instrument.

(**F**) Particle size distribution and numbers of EVs from mouse hepatocytes treated with Veh or 400 μM PA for 24 hours were assessed using a qNANO instrument.

(G) The uptake of fluorescently labeled EVs in MC38 and HCT116 cells was examined. EVs were obtained from mouse PHCs and Huh7 cells treated with PA and then labeled with PKH26 (red) and PKH67 (green), respectively. Fluorescently labeled EVs were incubated with MC38 or HCT116 cells for 24 hours followed by assessing the uptake of EVs through microscope **(left)** or Flow cytometry **(right)**. Scale bar, 50 nm.

(**H**) MC38 or HCT116 cells were treated with vehicle (Control) or EVs from cells treated with vehicle (Veh-EV) or 400 μM PA (PA-EV) for 48 hours, and then colony-forming assays were performed and quantified (n=4/group).

(**I**) In vitro cell migration and invasion assay. MC38 or HCT116 cells were treated with vehicle (Control), Veh-EV, or PA-EV for 48 hours and then placed in the upper chamber. The migration and invasion to the lower chamber were quantified (n=4/group).

(**J**) *Rab27a*, *Rab27b*, and *Smpd3* mRNA expression were examined by qRT-PCR. Mouse PHCs and Huh7 cells were treated with vehicle (BSA) or 400 μM PA for 24 hours (n=4/group).

(**K**) qRT-PCR for *Rab27a* mRNA in mouse PHCs. Cells were transfected with non-targeting siRNA control (siCon) or siRNA against *Rab27a* (si*Rab27a*) for 48 hours (n=3/group).

(**L**) EV particle numbers were counted using a qNANO instrument. Hepatocytes were transfected with siCon or si*Rab27a* for 48 hours followed by treated with 40 μM PA for 24 hours. EVs were purified from supernatants of these cells (n=3/group).

(**M**) Protocol for in vivo adenovirus-mediated delivery of shRNA. After 6 weeks of LFD or HFD feeding, adenovirus expressing either sh*Rab27a* or shCon ($1x10^9$ pfu/mouse) was administered intravenously. These adenovirus vectors contained genes expressing GFP. For experiment 1 (Exp #1), liver and serum samples were harvested 48 hours after adenoviral inoculation (n=5/group). For experiment 2 (Exp #2), MC38 cells ($1x10^5$ cells/mouse) were injected into the spleen 48 hours after adenoviral inoculation; liver and serum samples were harvested 12 days later (n=8-9/group).

(N) Oil Red O staining of liver samples from Exp #2. Representative images and quantifications.

(O) Images of efficacy of adenovirus infection by assessment of GFP expression. Both shCon and sh*Rab27a* exclusively infected hepatocytes and not tumor cells.
(P) Hepatic *Rab27a* mRNA expression in non-tumor livers from Exp #1.
(Q) EV particle numbers in serum samples collected from Exp #1.
(**R**) After 6 weeks of LFD or HFD feeding, adenovirus expressing short hairpin RNA (shRNA) for *Rab27a* (sh*Rab27a*) or a scrambled-shRNA control (shCon) was administered intravenously to mice. CMT93 cells were injected into the spleen 48 hours after adenoviral vector administration (n=9-10/group).
Representative macroscopic images. Scale bar, 1 cm. Number of metastatic tumors, and maximum tumor size.
(**S**) Adenovirus expressing *Rab27a* (Ad-*Rab27a*) or a control adenovirus (Ad-Con) was administered intravenously to mice. MC38 cells were injected into the spleen 48 hours after adenoviral vector administration (n=8-9/group).
Macroscopic images. Scale bar, 1 cm. EV particle numbers in mouse serum. Hepatic *Rab27a* mRNA expression in non-tumor liver tissues. Number of metastatic tumors, and maximum tumor size.
(**T**) Protocol for in vivo EV administrations. EVs were extracted from PHCs treated with vehicle (Veh-EV) or 400 μM PA (PA-EV) for 48 hours. After 6 weeks of LFD or HFD feeding, MC38 cells were injected into the spleen (n=8/group). 100 μg of EVs were administered intravenously to mice on day 0, 5, and 10 after tumor inoculations.
(**U**) Macroscopic images. Scale bar, 1 cm. Number of metastatic tumors, and maximum tumor size.
Data shown as mean ± SEM (F,H-L,N,P-S,U). Significance determined by two-tailed Student's *t*-test (F,J-L,S,U) or one-way ANOVA with Tukey's *post hoc* analysis (H,I,N,P,Q,R).

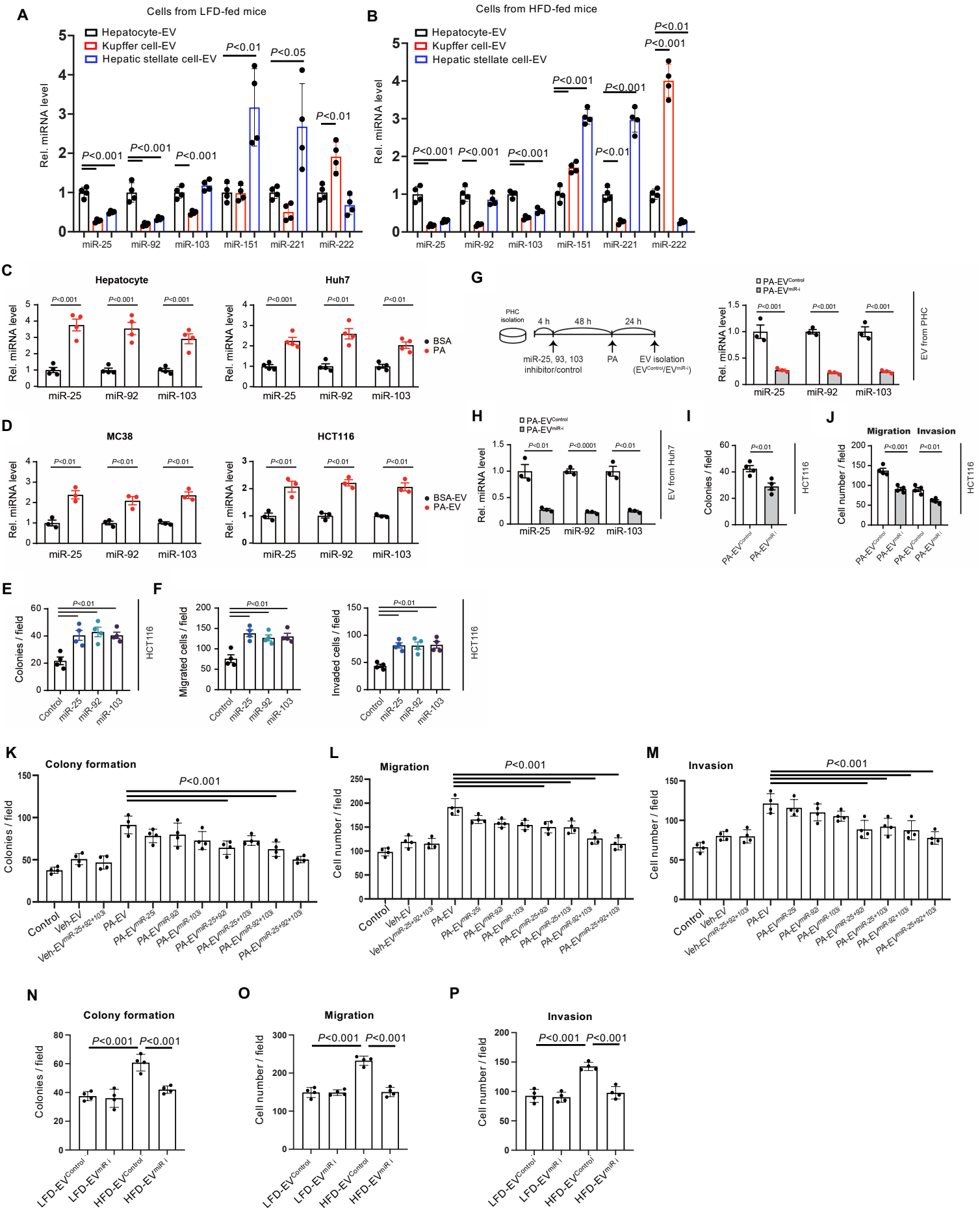
A
Cells from LFD-fed mice
Hepatocyte-EV
Kupffer cell-EV
Hepatic stellate cell-EV
Rel. miRNA level
miR-25
miR-92
miR-103
miR-151
miR-221
miR-222
B
Cells from HFD-fed mice
C
Hepatocyte
Huh7
BSA
PA
D
MC38
HCT116
BSA-EV
PA-EV
E
Colonies / field
HCT116
Control
F
Migrated cells / field
Invaded cells / field
G
PHC isolation
4 h
48 h
24 h
miR-25, 93, 103 inhibitor/control
PA
EV isolation (EVControl/EVmiR-i)
EV from PHC
H
EV from Huh7
I
J
Migration
Invasion
Cell number / field
K
Colony formation
Control
Veh-EV
PA-EV
L
Migration
M
Invasion
N
Colony formation
LFD-EVControl
LFD-EVmiR-i
HFD-EVControl
HFD-EVmiR-i
O
Migration
P
Invasion

Fig. S2

Figure S2. MiRNAs Are the Functional Extracellular Vesicle Contents That Aggravate Colorectal Cancer Growth in Fatty Liver, Related to Figure 2

(**A,B**) qRT-PCR assay for miR-25, miR-92, miR-103, miR-151, miR-221, miR-222 in EVs from primary hepatocytes, Kupffer cells, and hepatic stellate cells of mice fed a LFD (A) or a HFD (B) for 6 weeks. (n=4/group).

(C) qRT-PCR assay for miR-25, miR-92, and miR-103 in mouse hepatocytes and Huh7 cells treated with vehicle (BSA) or 400 μM PA for 24 hours (n=4/group).

(D) qRT-PCR assay for miR-25, miR-92, and miR-103 in MC38 cells or HCT116 cells. EVs were obtained from mouse PHCs and Huh7 cells treated with vehicle (BSA) or 400 □M PA for 24 hours and MC38 and HCT116 cells were then treated with EVs for 48 hours, respectively.

(**E**) Colony formation assay. HCT116 cells were transfected with negative control miRNA (Control), miR-25, miR-92, and miR-103 mimics (50 nM each) for 48 hours followed by performing colony formation assay. The average colony numbers per field are shown (n=4/group).

(**F**) Transwell cell migration and invasion assay. HCT116 cells were transfected with negative control (Control) or with miR-25, miR-92, or miR-103 mimics (50 nM each) for 48 hours followed by placing cells on the upper chamber. Quantification of migrated and invaded cells (n=4/group).

(**G**) Protocol for in vitro transfection of a combination of antagomiRs for miR-25, miR-92 and miR-103. Four hours after mouse primary hepatocytes (PHC) seeding, cells were transfected with a combination of three antagomiRs or a negative control antagomiR (100 nM each) for 48 hours. Then, cells were treated with 400 μM PA for an additional 24 hours. EVs were collected from the supernatants of PHCs (PA-$EV^{miR\text{-}i}$ or PA-$EV^{Control}$). EV miRNAs were measured by qRT-PCR assay (n=3/group).

(**H**) In a similar protocol as **(G)**, four hours after seeding, Huh7 cells were transfected with a combination of three antagomiRs or a negative control antagomir for 48 hours. Then, cells were treated with 400 μM PA for an additional 24 hours. EVs were collected from the supernatants of HuH7 cells (PA-$EV^{miR\text{-}i}$ or PA-$EV^{Control}$). EV miRNAs were determined by qRT-PCR assay (n=3/group).

(**I**) Colony-forming assay. HCT116 cells were treated with PA-$EV^{miR\text{-}i}$ or PA-$EV^{Control}$ (100 μg/ml) for 48 hours followed by performing colony formation assay (n=4/group).

(**J**) Transwell migration and invasion assay. HCT116 cells were treated with medium containing PA-$EV^{miR\text{-}i}$ or PA-$EV^{Control}$ (100 μg/ml) for 48 hours and then placed in the top chamber. The migration and invasion to the lower chamber were assessed (n=4/group).

(**K**) The effect of EVs with single or combinations of 2 antagomiRs for miR-25, miR-92, and miR-103 on MC38 cells. Four hours after mouse PHC seeding, cells were transfected with single or combinations of 2 or 3 antagomiRs (100 nM each) for 48 hours. Then, cells were treated with vehicle (BSA) or 400 μM PA for an additional 24 hours. EVs were collected from the supernatants of PHCs (Veh-$EV^{miR\text{-}i}$ or PA-$EV^{miR\text{-}i}$). Colony-forming assay. MC38 cells were

treated with various EVs (100 μg/ml) for 48 hours followed by performing colony formation assay (n=4/group).
(**L,M**) Transwell migration (L) and invasion (M) assay. MC38 cells were treated with medium containing various EVs (100 μg/ml) for 48 hours and then placed in the top chamber. The migration and invasion to the lower chamber were assessed (n=4/group).
(**N**) The effects of EVs from PHC isolated from LFD or HFD-fed mice on MC38 cells. Four hours after the seeding of PHC from LFD or HFD-fed mice, cells were transfected with a combination of three antagomiRs or a negative control antagomiR (100 nM each) for 48 hours. EVs were collected from the supernatants of PHC (LFD-$EV^{Control}$, LFD-$EV^{miR\text{-}i}$, HFD-$EV^{Control}$, or HFD-$EV^{miR\text{-}i}$). Colony-forming assay. MC38 cells were treated with LFD-$EV^{Control}$, LFD-$EV^{miR\text{-}i}$, HFD-$EV^{Control}$, or HFD-$EV^{miR\text{-}i}$ (100 μg/ml) for 48 hours followed by performing colony formation assay (n=4/group).
(**O,P**) Transwell migration (O) and invasion (P) assay. MC38 cells were treated with medium containing LFD-$EV^{Control}$, LFD-$EV^{miR\text{-}i}$, HFD-$EV^{Control}$, or HFD-$EV^{miR\text{-}i}$ (100 μg/ml) for 48 hours and then placed in the top chamber. The migration and invasion to the lower chamber were assessed (n=4/group).
Data are shown as mean ± SEM (A-P). Data were analyzed by two-tailed Student's *t*-test (C,D,G-J) or one-way ANOVA with Tukey's *post hoc* analysis (A,B,E,F,K-P).

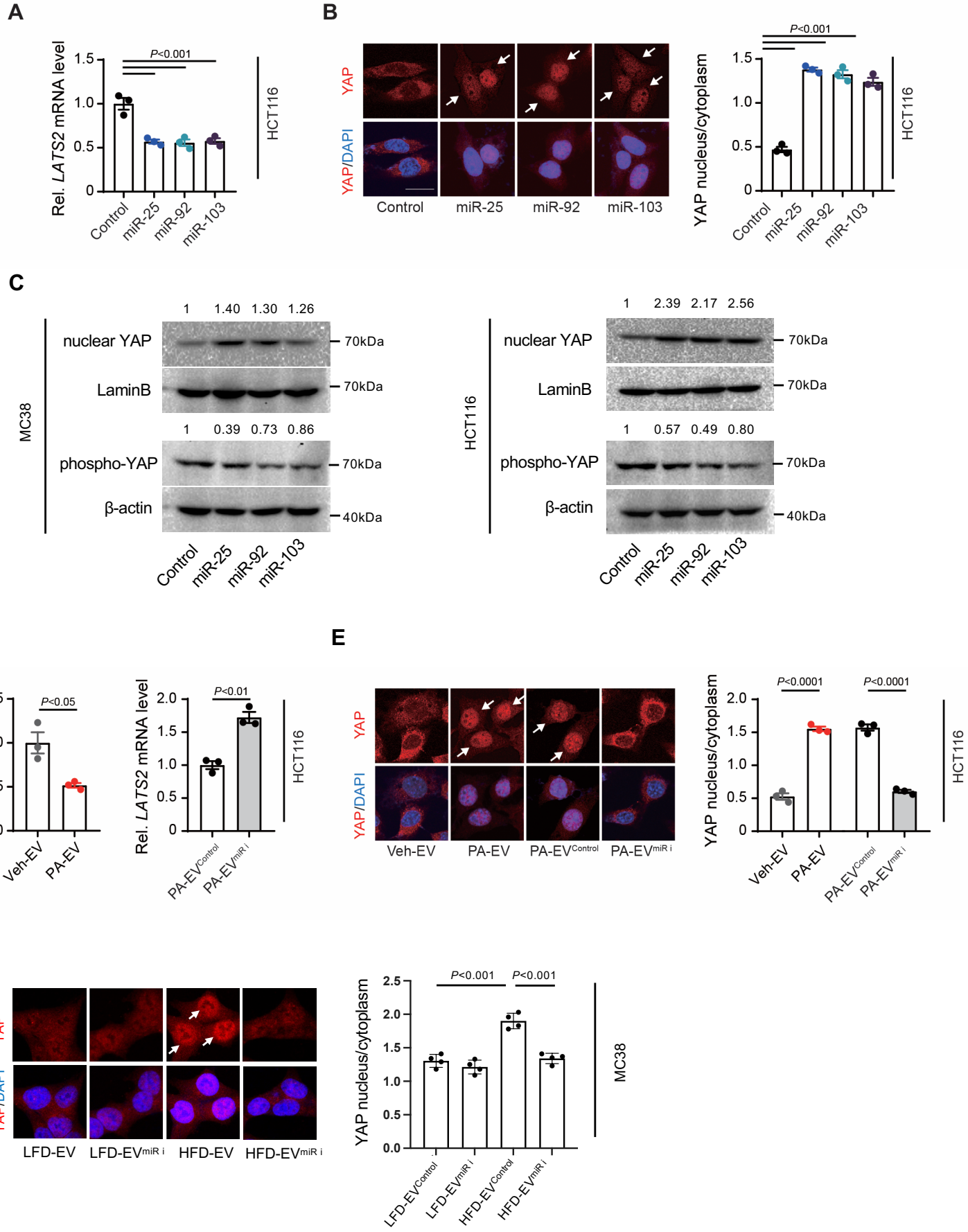
A
Rel. LATS2 mRNA level
P<0.001
HCT116
Control
miR-25
miR-92
miR-103
B
YAP
YAP/DAPI
YAP nucleus/cytoplasm
C
MC38
HCT116
nuclear YAP
LaminB
phospho-YAP
β-actin
70kDa
40kDa
1 1.40 1.30 1.26
1 0.39 0.73 0.86
1 2.39 2.17 2.56
1 0.57 0.49 0.80
D
P<0.05
P<0.01
Veh-EV
PA-EV
PA-EVControl
PA-EVmiR i
E
P<0.0001
F
LFD-EV
LFD-EVmiR i
HFD-EV
HFD-EVmiR i
P<0.001
MC38

Fig. S3

Figure S3. Extracellular vesicle-miRNAs Promote YAP Activation in Colorectal Cancer Cells, Related to Figure 3

(**A**) qRT-PCR assay for *LATS2* in the lysates of HCT116 cells transfected with negative control miRNA or with miR-25, miR-92, or miR-103 mimics (50 nM each) for 48 hours (n=3/group).
(**B**) HCT116 cells were transfected with negative control miRNA or with miR-25, miR-92, or miR-103 mimics (50 nM each) for 48 hours. The localization of YAP in HCT116 cells was examined. Representative immunofluorescence staining images (left). Corresponding nuclear/cytoplasmic YAP ratios are shown (right) (n=3/group). Scale bar, 10 nm.
(**C**) Immunoblots for nuclear YAP in nuclear fractions and phospho-YAP in whole cell lysates from MC38 and HCT116 cells treated with negative control miRNA or with miR-25, miR-92, or miR-103 mimics (50 nM each) for 48 hours.
(**D**) qRT-PCR assay for *LATS2* in the lysates of HCT116 cells treated with EVs. EVs were isolated from the supernatants of hepatocytes treated with vehicle (Veh-EV) or 400 μM PA (PA-EV) for 24 hours (left), or hepatocytes transfected with antagomiRs for miR-25, miR-92, and miR-103 (PA-$EV^{miR\text{-}i}$), or a control antagomiR (PA-$EV^{Control}$) for 48 hours followed by the treatment with 400 μM PA for 24 hours (right) (n=3/group).
(**E**) EVs were isolated from the supernatants of Huh7 cells treated with vehicle (Veh-EV) or 400 μM PA (PA-EV) for 24 hours, or Huh7 cells transfected with antagomiRs for miR-25, miR-92, and miR-103 (PA-$EV^{miR\text{-}i}$), or a control antagomiR (PA-$EV^{Control}$) for 48 hours followed by the treatment with 400 μM PA for 24 hours. The localization of YAP in HCT116 cells is shown. Representative immunofluorescence staining images (left). Corresponding nuclear/cytoplasmic YAP ratios are shown (right) (n=3/group).
(**F**) The effect of EVs from PHC isolated from LFD or HFD-fed mice on YAP nuclear translocation in MC38 cells. Four hours after the seeding of PHC from LFD or HFD-fed mice, cells were transfected with a combination of three antagomiRs or a negative control antagomiR (100 nM each) for 48 hours. EVs were collected from the supernatants of PHC (LFD-$EV^{Control}$, LFD-$EV^{miR\text{-}i}$, HFD-$EV^{Control}$, or HFD-$EV^{miR\text{-}i}$). (n=4/group). Based on immunofluorescence staining images for YAP, nuclear/cytoplasmic YAP ratios were analyzed. Data shown as mean ± SEM (A,B,D-F). Significance determined by one-way ANOVA with Tukey's *post hoc* analysis (A,B,F) or two-tailed Student's *t*-test (D,E).

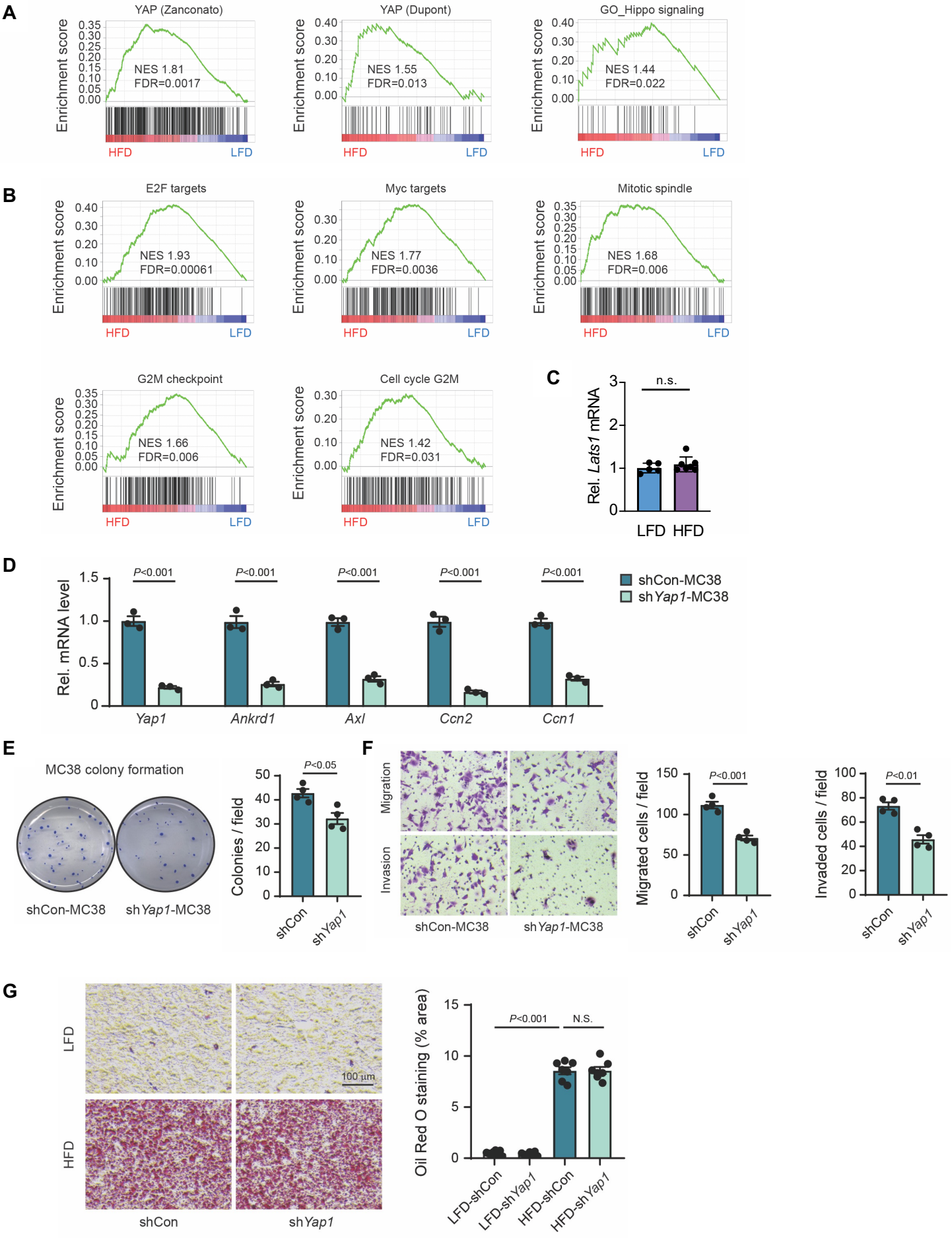
A
YAP (Zanconato)
NES 1.81
FDR=0.0017
YAP (Dupont)
NES 1.55
FDR=0.013
GO_Hippo signaling
NES 1.44
FDR=0.022
Enrichment score
HFD
LFD
B
E2F targets
NES 1.93
FDR=0.00061
Myc targets
NES 1.77
FDR=0.0036
Mitotic spindle
NES 1.68
FDR=0.006
G2M checkpoint
NES 1.66
FDR=0.006
Cell cycle G2M
NES 1.42
FDR=0.031
C
n.s.
Rel. Lats1 mRNA
LFD HFD
D
P<0.001
shCon-MC38
shYap1-MC38
Rel. mRNA level
Yap1
Ankrd1
Axl
Ccn2
Ccn1
E
MC38 colony formation
shCon-MC38
shYap1-MC38
P<0.05
Colonies / field
shCon
shYap1
F
Migration
Invasion
shCon-MC38
shYap1-MC38
P<0.001
Migrated cells / field
P<0.01
Invaded cells / field
G
LFD
HFD
100 μm
shCon
shYap1
Oil Red O staining (% area)
P<0.001
N.S.
LFD-shCon
LFD-shYap1
HFD-shCon
HFD-shYap1

Fig. S4

Figure S4. YAP Activity Contributes to Colorectal Cancer Liver Metastasis Enhanced by Non-Alcoholic Fatty Liver Disease, Related to Figure 4

(**A, B**) RNA-seq was performed using tumor samples from procedures described in Figure 1A (n=5/group). GSEA shows that several previously published YAP target gene sets (A) and oncogenic gene sets (B) are enriched in tumors from HFD-fed mice compared with tumors from LFD-fed mice.

(**C**) qRT-PCR assays for *Lats1* in tumor samples from mice fed a LFD or a HFD (n=5-7/group).

(**D**) qRT-PCR assays for *Yap1* and its target genes (*Ankrd1, Axl1, Ccn2,* and *Ccn1*) were performed for MC38 cells stably transfected with scrambled control shRNA (shCon-MC38) or shRNA against *Yap1* (sh*Yap1*-MC38) (n=3/group).

(E,F) The effect of stable knockdown of *Yap1* in MC38 cells on (E) colony formation and (F) cell migration and invasion (n=4/group).

(**G**) Oil Red O staining of livers from the in vivo experiment (LFD-shCon, LFD-sh*Yap1*, HFD-shCon, and HFD-sh*Yap1*). Representative images (left) and their quantification (right). Data shown as mean ± SEM (C-G). Significance determined by two-tailed Student's *t*-test (C-F) or one-way ANOVA with Tukey's *post hoc* analysis (G). n.s., not significant.

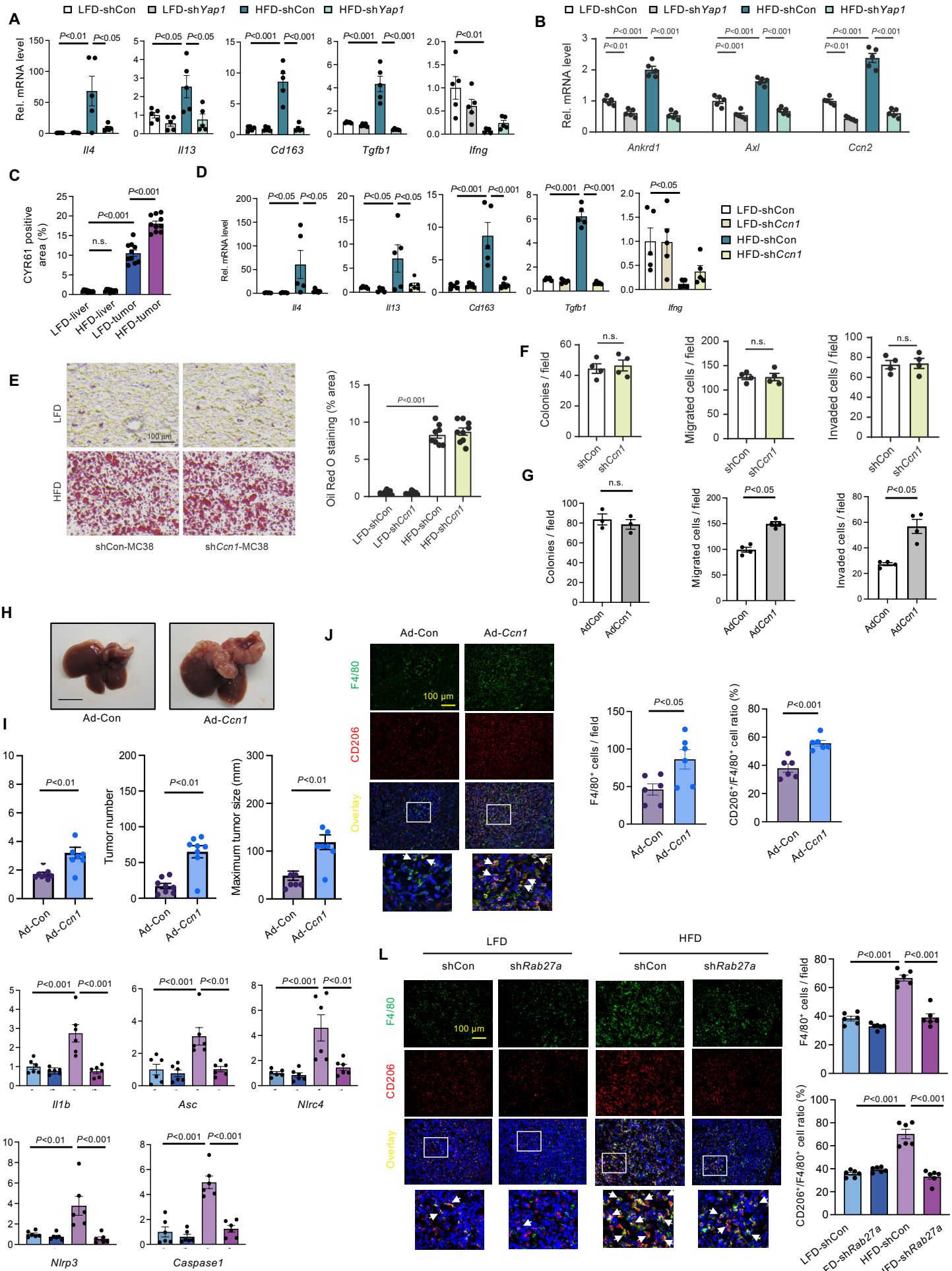
A
LFD-shCon
LFD-shYap1
HFD-shCon
HFD-shYap1
Rel. mRNA level
Il4
Il13
Cd163
Tgfb1
Ifng
B
Ankrd1
Axl
Ccn2
C
CYR61 positive area (%)
n.s.
LFD-liver
HFD-liver
LFD-tumor
HFD-tumor
D
LFD-shCon
LFD-shCcn1
HFD-shCon
HFD-shCcn1
E
LFD
HFD
100 μm
shCon-MC38
shCcn1-MC38
Oil Red O staining (% area)
F
Colonies / field
Migrated cells / field
Invaded cells / field
shCon
shCcn1
G
AdCon
AdCcn1
H
Ad-Con
Ad-Ccn1
I
Liver weight (g)
Tumor number
Maximum tumor size (mm)
J
F4/80
CD206
Overlay
F4/80+ cells / field
CD206+/F4/80+ cell ratio (%)
K
Il1b
Asc
Nlrc4
Nlrp3
Caspase1
L
LFD
HFD
shCon
shRab27a
LFD-shRab27a
HFD-shRab27a

Fig. S5

Figure S5. CYR61 Is the Critical Factor for YAP-Mediated Liver Metastasis by Induction of an Immunosuppressive Tumor Microenvironment, Related to Figure 5

(**A**) qRT-PCR assays for M1/M2-related genes (*Il4, Il13, Cd163, Tgfb1,* and *Ifng*) (n=5/group) in tumor samples from Figure 5A (LFD-shCon, LFD-sh*Yap1*, HFD-shCon, and HFD-sh*Yap1*).

(**B**) qRT-PCR assays for YAP transcriptional target genes (*Ankrd1, Axl1,* and *Ccn2*) (n=5/group) in tumor samples from Figure 5D (LFD-shCon, LFD-sh*Yap1*, HFD-shCon, and HFD-sh*Yap1*).

(**C**) Immunohistochemistry for CYR61 and quantification of CYR61-positive area of non-tumor liver tissues and tumors from mice fed a LFD or a HFD (n=10/group).

(**D**) qRT-PCR assays for M1/M2-related genes (*Il4, Il13, Cd163, Tgfb1,* and *Ifng*) (n=5/group) in tumor samples from Figure 5F (LFD-shCon, LFD-sh*Ccn1*, HFD-shCon, and HFD-sh*Ccn1*).

(**E**) Oil Red O staining of livers from the in vivo experiment (LFD-shCon, LFD-sh*Ccn1*, HFD-shCon, and HFD-sh*Ccn1*). Representative images (left), and their quantification (right).

(F) The effect of stable knockdown of CYR61 in MC38 cells on colony formation and cell migration and invasion (n=4/group).

(G) The effect of overexpression of CYR61 in MC38 cells on colony formation (n=3/group) and cell migration and invasion (n=4/group).

(**H-J**) Adenovirus expressing *Ccn1* (Ad*Ccn1*) or a control adenovirus (AdCon) was administered intravenously to mice. MC38 cells were injected into the spleen 48 hours after adenoviral vector administration (n=8/group). (H) Macroscopic images. Scale bar, 1 cm. (I) Liver weight. Number of metastatic tumors, and maximum tumor size. (J) Co-localization of F4/80 and CD206 in tumors from Figure S5H. Representative immunofluorescent images. Quantification of $F4/80^+$ cells and ratio of $CD206^+/F4/80^+$.

(**K**) qRT-PCR assays for inflammasome-related genes (*Il1b, Asc, Nlrp3, Nlrc4,* and *Caspase-1*) (n=6/group) in non-tumor liver tissues and tumor samples from Figure 1K-N (LFD-shCon, LFD-sh*Rab27a*, HFD-shCon, and HFD-sh*Rab27a*).

(**L**) Co-localization of F4/80 and CD206 in tumors from Figure 1M. Representative immunofluorescent images. Quantification of $F4/80^+$ cells and ratio of $CD206^+/F4/80^+$.

Data shown as mean ± SEM (A-L). Significance determined by one-way ANOVA with Tukey's *post hoc* analysis (A-E,K,L) or two-tailed Student's *t*-test (F,G,I,J). n.s., not significant.

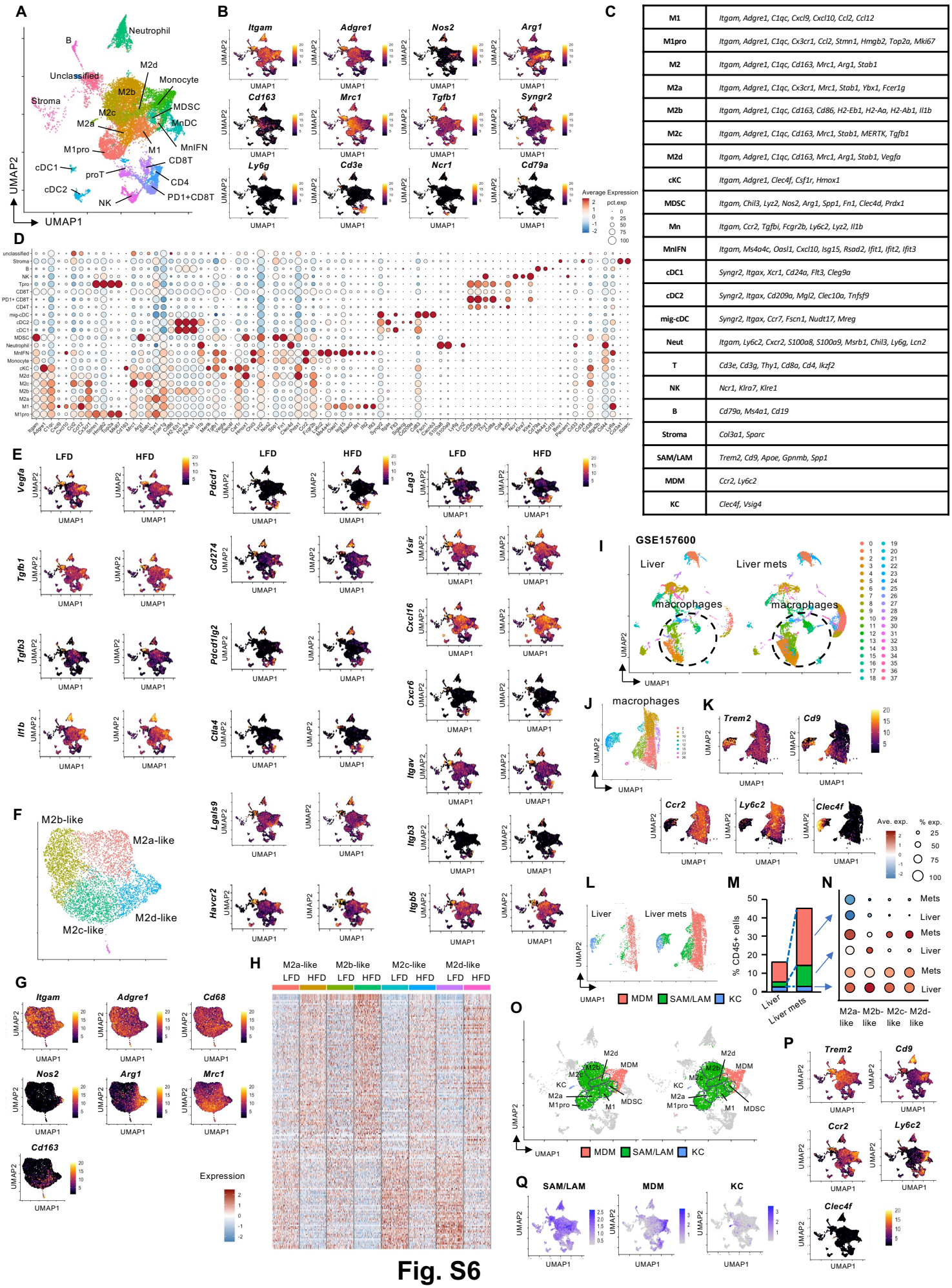
A
Neutrophil
B
M2d
Unclassified
Monocyte
M2b
Stroma
MDSC
M2c
M2a
MnDC
MnIFN
M1pro
M1
CD8T
cDC1
proT
CD4
cDC2
PD1+CD8T
NK
UMAP2
UMAP1
B
Itgam
Adgre1
Nos2
Arg1
Cd163
Mrc1
Tgfb1
Syngr2
Ly6g
Cd3e
Ncr1
Cd79a
UMAP1
UMAP2
Average Expression
pct.exp
C
M1 | Itgam, Adgre1, C1qc, Cxcl9, Cxcl10, Ccl2, Ccl12
M1pro | Itgam, Adgre1, C1qc, Cx3cr1, Ccl2, Stmn1, Hmgb2, Top2a, Mki67
M2 | Itgam, Adgre1, C1qc, Cd163, Mrc1, Arg1, Stab1
M2a | Itgam, Adgre1, C1qc, Cx3cr1, Mrc1, Stab1, Ybx1, Fcer1g
M2b | Itgam, Adgre1, C1qc, Cd163, Cd86, H2-Eb1, H2-Aa, H2-Ab1, Il1b
M2c | Itgam, Adgre1, C1qc, Cd163, Mrc1, Stab1, MERTK, Tgfb1
M2d | Itgam, Adgre1, C1qc, Cd163, Mrc1, Arg1, Stab1, Vegfa
cKC | Itgam, Adgre1, Clec4f, Csf1r, Hmox1
MDSC | Itgam, Chil3, Lyz2, Nos2, Arg1, Spp1, Fn1, Clec4d, Prdx1
Mn | Itgam, Ccr2, Tgfbi, Fcgr2b, Ly6c2, Lyz2, Il1b
MnIFN | Itgam, Ms4a4c, Oasl1, Cxcl10, Isg15, Rsad2, Ifit1, Ifit2, Ifit3
cDC1 | Syngr2, Itgax, Xcr1, Cd24a, Flt3, Cleg9a
cDC2 | Syngr2, Itgax, Cd209a, Mgl2, Clec10a, Tnfsf9
mig-cDC | Syngr2, Itgax, Ccr7, Fscn1, Nudt17, Mreg
Neut | Itgam, Ly6c2, Cxcr2, S100a8, S100a9, Msrb1, Chil3, Ly6g, Lcn2
T | Cd3e, Cd3g, Thy1, Cd8a, Cd4, Ikzf2
NK | Ncr1, Klra7, Klre1
B | Cd79a, Ms4a1, Cd19
Stroma | Col3a1, Sparc
SAM/LAM | Trem2, Cd9, Apoe, Gpnmb, Spp1
MDM | Ccr2, Ly6c2
KC | Clec4f, Vsig4
D
unclassified
Stroma
B
NK
Tpro
CD8T
PD1+ CD8T
CD4T
mig-cDC
cDC2
cDC1
MDSC
Neutrophil
MnIFN
Monocyte
cKC
M2d
M2c
M2b
M2a
M1
M1pro
E
LFD
HFD
Vegfa
Pdcd1
Lag3
Tgfb1
Cd274
Vsir
Tgfb3
Pdcd1lg2
Cxcl16
Il1b
Cxcr6
Cd4
Itgav
Lgals9
Itgb3
Havcr2
Itgb5
F
M2b-like
M2a-like
M2d-like
M2c-like
G
Itgam
Adgre1
Cd68
Nos2
Arg1
Mrc1
Cd163
Expression
H
M2a-like
M2b-like
M2c-like
M2d-like
LFD
HFD
I
GSE157600
Liver
Liver mets
macrophages
J
macrophages
K
Trem2
Cd9
Ccr2
Ly6c2
Clec4f
Ave. exp.
% exp.
L
Liver
Liver mets
MDM
SAM/LAM
KC
M
% CD45+ cells
Liver
Liver mets
N
Mets
Liver
M2a-like
M2b-like
M2c-like
M2d-like
O
M2d
MDM
M2b
M2c
KC
M2a
M1pro
M1
MDSC
P
Trem2
Cd9
Ccr2
Ly6c2
Clec4f
Q
SAM/LAM
MDM
KC

Fig. S6

Figure S6. Non-Alcoholic Fatty Liver Disease Contributes to Tumor-Promoting Tumor-associated Macrophages and CD8 T Cell Phenotypes in the Tumor Microenvironment of Colorectal Cancer Liver Metastasis, Related to Figure 6

(**A**) Determination of tumor-infiltrating immune cell populations. UMAP of single-cell RNA-seq analyses from 15,141 $CD45^+$ immune cells showing 22 clusters determined by integrated analysis, colored by cluster. Cells were isolated from metastatic liver tumors of LFD-fed and HFD-fed mice (n=3/group).

(B) Expression levels of key cluster-identification genes.

(C) Key cluster-identification genes for each cluster.

(D) Dot plot for key cluster signatures (columns) by specific subpopulations (rows) based on Figure S6C. Dot size represents the cell fraction within each subpopulation. Fill color indicates average expression.

(E) Expression levels of key tumor-promoting and immunomodulatory genes mapped on the corresponding UMAP embedding.

(F, G) UMAPs of re-clustered M2 macrophages and expression of key identification genes for clustering M2 subpopulations.

(H) Heatmap of four M2 subpopulations from tumors of LFD-fed and HFD-fed mice at a single-cell level.

(**I**) UMAP of single-cell RNA-seq analyses from GSE157600 showing 27 clusters determined by integrated analysis, colored by cluster. The data contain RNA-seq data from single cells from the normal liver (Liver) and the liver tissues with MC38 tumors (Liver mets).

(J-L) (J) UMAP of re-clustered macrophages from GSE157600 and (K) expression of key identification genes for clustering the subpopulations of myeloid-derived macrophages (MDM), scar or lipid-associated macrophages (SAM/LAM), and Kupffer cells (KC). (L) UMAP of re-clustered macrophages from Liver and Liver mets.

(M,N) (M) Bar plots depict the proportion of MDM, SAM/LAM, and KC in $CD45^+$ cells in Liver and Liver mets. (N) Dot plot for expression of signatures of M2 subpopulations (columns) by macrophage subpopulations (MDM, SAM/LAM, KC) from livers with or without tumors (rows). Dot size represents the cell fraction within each cell population. Fill color indicates average expression.

(O-Q) (O) UMAPs of clustered SAM/LAM, MDM, and KC in tumors of LFD-fed and HFD-fed mice. (P) Expression of key identification genes for SAM/LAM, MDM, and KC in tumors of LFD-fed and HFD-fed mice. (Q) Summarized expression levels of cell type specific gene signatures for SAM/LAM, MDM, and KC.

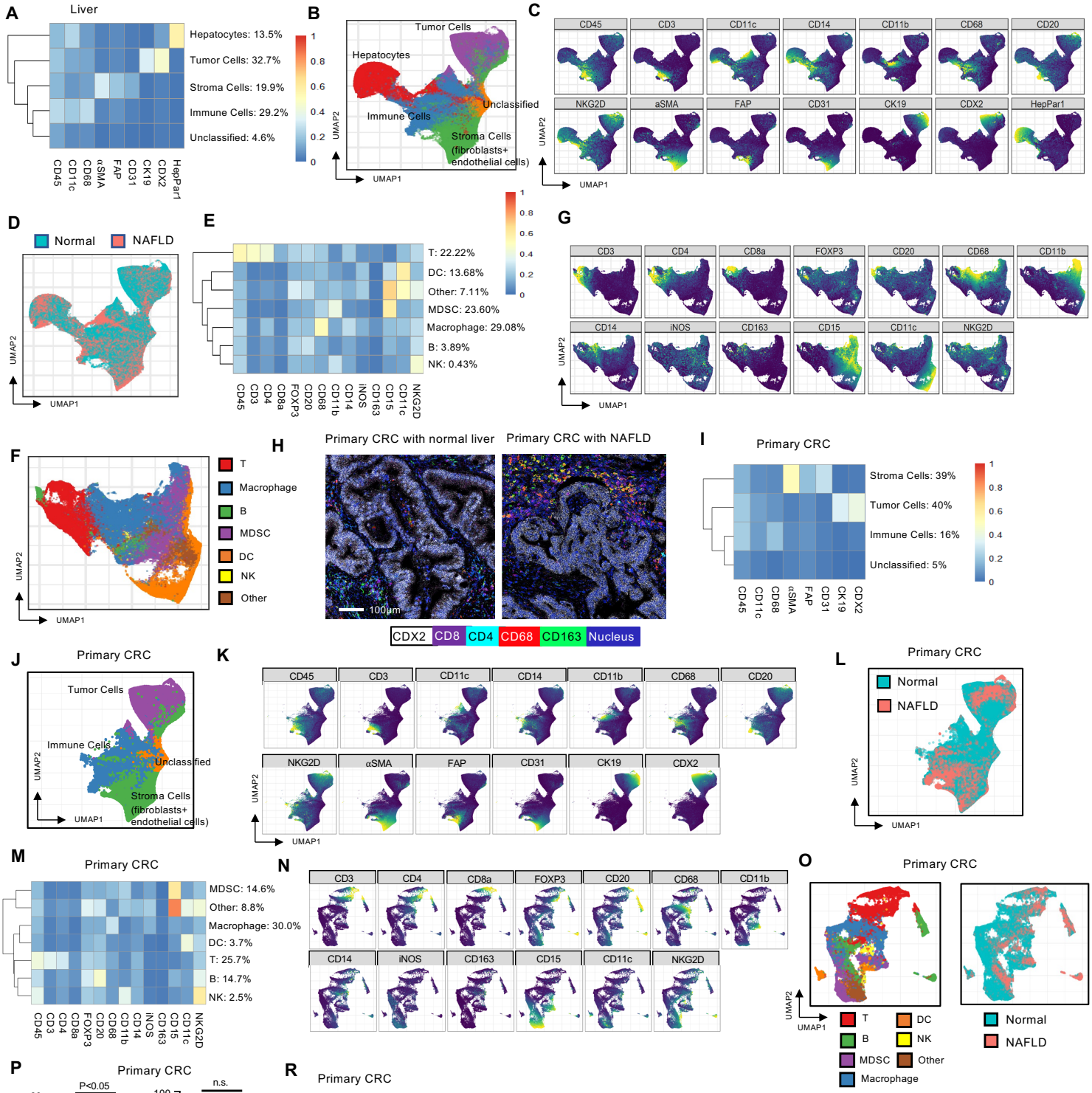
A
Liver
Hepatocytes: 13.5%
Tumor Cells: 32.7%
Stroma Cells: 19.9%
Immune Cells: 29.2%
Unclassified: 4.6%
CD45 CD11c CD68 αSMA FAP CD31 CK19 CDX2 HepPar1
B
Tumor Cells
Hepatocytes
Unclassified
Immune Cells
Stroma Cells (fibroblasts+ endothelial cells)
UMAP1 UMAP2
C
CD45 CD3 CD11c CD14 CD11b CD68 CD20
NKG2D αSMA FAP CD31 CK19 CDX2 HepPar1
UMAP1 UMAP2
D
Normal NAFLD
UMAP1 UMAP2
E
T: 22.22%
DC: 13.68%
Other: 7.11%
MDSC: 23.60%
Macrophage: 29.08%
B: 3.89%
NK: 0.43%
CD45 CD3 CD4 CD8a FOXP3 CD20 CD68 CD11b CD14 iNOS CD163 CD15 CD11c NKG2D
G
CD3 CD4 CD8a FOXP3 CD20 CD68 CD11b
CD14 iNOS CD163 CD15 CD11c NKG2D
UMAP1 UMAP2
F
T
Macrophage
B
MDSC
DC
NK
Other
UMAP1 UMAP2
H
Primary CRC with normal liver
Primary CRC with NAFLD
100μm
CDX2 CD8 CD4 CD68 CD163 Nucleus
I
Primary CRC
Stroma Cells: 39%
Tumor Cells: 40%
Immune Cells: 16%
Unclassified: 5%
CD45 CD11c CD68 αSMA FAP CD31 CK19 CDX2
J
Primary CRC
Tumor Cells
Immune Cells
Unclassified
Stroma Cells (fibroblasts+ endothelial cells)
UMAP1 UMAP2
K
CD45 CD3 CD11c CD14 CD11b CD68 CD20
NKG2D αSMA FAP CD31 CK19 CDX2
UMAP1 UMAP2
L
Primary CRC
Normal
NAFLD
UMAP1 UMAP2
M
Primary CRC
MDSC: 14.6%
Other: 8.8%
Macrophage: 30.0%
DC: 3.7%
T: 25.7%
B: 14.7%
NK: 2.5%
CD45 CD3 CD4 CD8a FOXP3 CD20 CD68 CD11b CD14 iNOS CD163 CD15 CD11c NKG2D
N
CD3 CD4 CD8a FOXP3 CD20 CD68 CD11b
CD14 iNOS CD163 CD15 CD11c NKG2D
O
Primary CRC
UMAP1 UMAP2
T
B
MDSC
Macrophage
DC
NK
Other
Normal
NAFLD
P
Primary CRC
P<0.05
n.s.
% M2 of total Mac
% M1 of total Mac
Normal NAFLD
R
Primary CRC
n.s.
% CD8T of total immune cells
% CD4T of total immune cells
Normal NAFLD
S
Primary CRC
Treg CD8T CD4T
Normal NAFLD
CD4 CD8a FOXP3
PD1 PDL1 LAG3 VISTA TIM3
Ave. exp.
high
low
% exp.
40 60 80 100
70 80 90 100
T
YAP (-) YAP (+)
P<0.001 P<0.001
Distance to nearest target cells (μm)
M2 CD8T
Q
Primary CRC
nonM1M2 M2 M1
Normal NAFLD
CD163 iNOS PDL1 VISTA Galectin9 TIM3
Ave. exp.
high
low
% exp.
25 50 75

Fig. S7

Figure S7. Increased YAP Activity and Immunosuppressive Tumor Microenvironment in Colorectal Cancer Liver Metastasis Patients with Non-Alcoholic Fatty Liver Disease, Related to Figure 7

(**A-G)** IMC analysis of TMA comprising patients with CRC liver metastasis with NAFLD (n=13) and without NAFLD (n=17; Normal).

(A) Heatmap of cell populations determined by key cluster-identification molecules from IMC analyses from 430,306 cells.

(B) UMAP from **(A)** showing five clusters determined by integrated analysis, colored by cluster.

(C) UMAPs of expression of key cluster-identification molecules.

(D) UMAPs colored by NAFLD condition.

(E) Heatmap of immune cell populations determined by key cluster-identification molecules from IMC analyses from 147,328 immune cells.

(F) UMAP from **(E)** showing seven clusters determined by integrated analysis, colored by cluster.

(G) UMAPs of expression of key immune cluster-identification molecules.

(H-T) IMC for TMA comprising primary CRC from liver metastasis patients with NAFLD (n=7) and without NAFLD (n=12; Normal).

(H) Representative IMC images for primary CRC for CDX2, CD8, CD4, CD68, and CD163 expression.

(I) Heatmap of cell populations determined by key cluster-identification molecules from IMC analyses from 308,551 cells.

(J) UMAP from **(I)** showing four clusters determined by integrated analysis, colored by cluster.

(K) UMAPs of expression of key cluster-identification molecules.

(L) UMAPs colored by NAFLD condition.

(M) Heatmap of immune cell populations determined by key cluster-identification molecules from IMC analyses from 63,419 immune cells.

(N) UMAPs of expression of key immune cluster-identification molecules.

(O) UMAP from **(M)** showing seven clusters determined by integrated analysis, colored by cluster (left). UMAP of immune cells, colored to distinguish normal and NAFLD conditions (right).

(P) Quantification of CD163-expressing (M2) and iNOS-expressing (M1) macrophages (Mac).

(Q) Dot plot for expression of key cluster-identification and immunomodulatory molecules (columns) by macrophage subpopulations from patients with or without NAFLD (rows). Dot size represents the cell fraction within each cell population. Fill color indicates average expression.

(R) Quantification of CD8 and CD4 T cells.

(S) Dot plot for expression of key cluster-identification and immunomodulatory molecules (columns) by T cell subpopulations in patients with or without NAFLD (rows). Dot size represents the cell fraction within each cell population. Fill color indicates average expression.

(T) Spatial analysis of IMC to measure the distances between immune cells (M2 macrophages or CD8 T cells) and primary CRC cells with and without YAP expression (n=130,364 cells). Data

shown as mean ± SEM (P,R) or mean ± SD (T). Significance determined by two-tailed Student's *t*-test (P,R,T).